CDMA System Design Through Asymptotic Analysis

Ezio Biglieri, *Fellow, IEEE*, Giuseppe Caire, *Member, IEEE*, and Giorgio Taricco, *Member, IEEE*

Abstract—We use results from the asymptotic analysis of code-division multiple access with random spreading as a tool for gaining insight and deriving design guidelines on practical system issues, inspired by the current UMTS/IMT2000 standardization process. In particular, we consider a simple synchronous single-cell system with perfect power control and linear detection, and we examine the following: 1) the optimal tradeoff between coding rate and spreading gain and 2) the comparison of different multirate schemes.

Our analysis shows that, for the sake of system spectral efficiency maximization, there exists a threshold E_b/N_0 below which the single-user matched filter (SUMF) is optimal (within the limits of our system model). As far as multirate schemes are concerned, we show that multicode and variable-spreading with SUMF detection are equivalent, while the former is uniformly better than the latter with linear minimum-mean-square error detection. Variable-spreading can perform very close to multicode if high-rate users are detected by observing the whole "low-rate" symbol interval. Finally, we compare the capacity regions of the multimodulation and multicode schemes versus the E_b/N_0 ratio.

Index Terms—CDMA system capacity, linear receivers, multirate CDMA, random spreading.

I. INTRODUCTION AND MOTIVATIONS

THE system capacity of code-division multiple access (CDMA) depends on several factors like user synchronism, the choice of spreading sequences, the partition of the overall bandwidth expansion between spreading gain and channel coding rate, the effects and statistics of multipath propagation channels, the geometry of cell coverage and sectorization, power control and power allocation schemes, the type of receiver (coherent, noncoherent, single-user, multiuser, linear, nonlinear) used at the base stations and at the user terminals.

Even by restricting the analysis to *oversimplified* single-cell synchronous CDMA systems with frequency-flat propagation channels, results depend on the set of spreading sequences and on the receiver scheme used.

The need to gain insight into the fundamental system design tradeoffs independently of the system fine structure motivates the asymptotic analysis based on random spreading sequences of [1]–[5]. In these works, the powerful theory of limiting eigenvalue distribution of large random matrices (see [6] and [7],

and references in [3] and [4]) is used to study the system capacity of single-cell synchronous CDMA under the assumption of random spreading sequences and *large systems*, i.e., when both the number of users K and the spreading gain L go to infinity, but the ratio $\alpha = K/L$ of users per chip converges to a constant. These results have been extended in [8] to the case of chip-synchronous, symbol-asynchronous systems, in [9] to the case of flat fading, in [10] to the case of multipath fading with nonideal channel estimation, and in [11] to the case of optimal (nonlinear) multiuser detection.

The main goal of this manuscript is to show how the theoretical results of [4] and [8] can be used to develop useful design guidelines for some practical issues of CDMA systems. This study is motivated by the debate around the standardization of UMTS/IMT2000 [12], [13] third-generation mobile communication systems, and in particular by the definition of a UMTS air interface for satellite personal communications [14]. In low-earth orbit satellite systems, because of the limited on-board power and the high carrier frequency, line-of-sight (LOS) propagation is necessary to close the link-budget. Multipath is negligible, so that the channel can be modeled as frequency flat. Users belonging to the same spot-beam are well isolated from interbeam interference by the radiation pattern of the spotbeam antenna. Power control is able to compensate for variations due to the relative motion of the user terminal and the spot-beam. Therefore, by neglecting the possible Rician fading and synchronization errors,[1] synchronous CDMA with perfect power control is not an unrealistic model (asynchronous interference generated by other satellites in LOS can be either taken into account by suitably dimensioning the background noise power spectral density or eliminated by some beam switching-off strategy).

We consider a coded system where the receiver of each user consists of a linear filter front-end, viz., either a single-user matched filter (SUMF) receiver or a linear minimum-mean-square error (LMMSE) receiver [7], followed by a single-user decoder. The key performance measure here is the signal-to-interference-plus-noise ratio (SINR) at the filter output. In fact, the users' quality of service (QoS) can be expressed in terms of a target SINR, depending on the user channel code.

This paper is organized as follows. In Section II, we review the synchronous CDMA system model and the main results of [4], which will be used throughout this paper. In Section III, we apply the asymptotic random spreading analysis to the investigation of the optimal tradeoff between coding rate and spreading gain. We take into account the influence of different

E. Biglieri and G. Taricco are with the Dipartimento di Elettronica, Politecnico di Torino, I-10129 Torino, Italy (e-mail: biglieri@polito.it; taricco@polito.it).

G. Caire is now with Mobile Communications Group, Institut Eurècom, 06904 Sophia Antipolis, France (e-mail: giuseppe.caire@eurecom.fr).

[1]Typically, the fraction of LOS to scattered received energy (Rician factor) is large ($\geq$10 dB) and quasi-synchronous transmission in the same beam is possible also in the uplink [14], [15].

pilot channel formats proposed for UMTS [12] to enable coherent detection. Pilot channels can be either multiplexed into the data symbols (pilot symbols) or superimposed to the data signal as an additional spread spectrum signal (pilot signals). In Section IV, we compare different multirate CDMA schemes [16]–[19] in terms of their asymptotic capacity region. Finally, in Section V, we outline the main findings of this research.

II. SYSTEM MODEL

We consider a single-cell synchronous direct-sequence CDMA system (DS-CDMA) with frequency-flat propagation and perfect power control, so that fading and deterministic path attenuation are perfectly compensated for. The receiver front-end is formed by a chip-matched filter followed by sampling at the chip rate. We let K and L denote the number of users and the spreading gain (number of chip per symbol), w_k, a_k, and $\mathbf{s}_k = (1/\sqrt{L})(s_{1,k}, \ldots, s_{L,k})^T$ denote the kth user complex amplitude (taking into account the carrier phase), modulation symbol, and spreading sequence, respectively. For each symbol interval, the receiver collects a vector $\mathbf{y}$ of L chip-rate samples, which can be written as [7]

$$\mathbf{y} = \mathbf{SWa} + \nu \qquad (1)$$

where $\mathbf{S} = [\mathbf{s}_1, \ldots, \mathbf{s}_K]$ is an $L \times K$ matrix whose columns are the user spreading sequences, $\mathbf{W} = \mathrm{diag}(w_1, \ldots, w_K), \mathbf{a} = (a_1, \ldots, a_K)^T$, and $\nu = (\nu_1, \ldots, \nu_L)$ is a complex circularly symmetric white Gaussian noise vector with per-component variance $E[|\nu_\ell|^2] = N_0$. Modulation symbols and spreading sequences have unit average energy, i.e., $E[|a_k|^2] = 1$ and $E[|\mathbf{s}_k|^2]$ for all k. The average received energy per symbol from user k is $\mathcal{E}_k = |w_k|^2$ and the user k signal-to-noise ratio (SNR) is given by $\gamma_k \triangleq \mathcal{E}_k/N_0$.

The receiver of each user k is formed by a linear filtering operation $z_k = \mathbf{h}_k^H \mathbf{y}$, followed by single-user decoding acting on the filter output. We consider SUMF and LMMSE receivers [7], defined by the filter vectors

$$\mathbf{h}_k = \begin{cases} w_k \mathbf{s}_k & \text{(SUMF)} \\ w_k \mathbf{R}_y^{-1} \mathbf{s}_k & \text{(LMMSE)} \end{cases} \qquad (2)$$

where $\mathbf{R}_y \triangleq \mathrm{cov}(\mathbf{y}) = \mathbf{SWW}^H\mathbf{S}^H + N_0\mathbf{I}$.

Following [4], we model the spreading sequences as random with independently, identically distributed (i.i.d.) complex circularly symmetric entries $s_{\ell,k}$, such that $E[s_{\ell,k}] = 0, E[|s_{\ell,k}|^2] = 1$, and $E[|s_{\ell,k}|^4] < \infty$. Let $\gamma_I^{(K)}$ be a random variable obtained by selecting at random with uniform probability the SNR of a user, i.e., $\Pr(\gamma_I^{(K)} = \gamma_k) = 1/K$, for all $k = 1, \ldots, K$. As $K \to \infty$, we assume that $\gamma_I^{(K)}$ converges in distribution to a random variable γ_I, with a given cumulative distribution function (cdf) $F_\gamma(x)$. Finally, we assume a *large system*, i.e., we let $K, L \to \infty$ while K/L is finite and converges to a given value α. Notice that the ratio K/L is the "channel load," measured in *users per chip*. Under the above conditions, the SINR at the output of an SUMF and an LMMSE receiver for a user with given SNR γ converges in

probability to the value β given by the following equations [4, Theorem 3.1 and Proposition 3.3]:

$$\beta = \begin{cases} \dfrac{\gamma}{1 + \alpha E[\gamma_I]} & \text{(SUMF)} \\ \dfrac{\gamma}{1 + \alpha E[\gamma\gamma_I/(\gamma + \gamma_I\beta)]} & \text{(LMMSE)}. \end{cases} \qquad (3)$$

Concerning the LMMSE case, β must be taken as the unique positive solution to the relevant equation and the uniqueness of this solution is proven in [4, Proposition 3.2].

III. CODING VERSUS SPREADING

The *system spectral efficiency* of a multiuser system is the number η of users $\times$ bits/s/Hz that the system is able to support subject to a given QoS constraint on the transmission of each user. We let R_b and W denote the bit rate (bits/second) of each user and the system bandwidth (Hertz), respectively. Then, we have $\eta = KR_b/W$. We assume also that users transmit at given power $\mathcal{P}$, so that $E_b/N_0 = (\mathcal{P}/R_b)/N_0$ is the same for all users.

In practical systems, a fraction ε of the transmission resource per user is dedicated to synchronization and channel estimation [12], [13]. In UMTS, two main techniques are considered: multiplexed pilot symbols and superimposed pilot signals. Going into the details of specific algorithms is out of the scope of this paper. However, experimental evidence shows that the quality of channel estimation provided by both the pilot symbols and pilot signals technique depends mainly on ε, and provide similar results for the same ε [15]. Then, apart from practical implementation considerations, the two techniques are equivalent as far as channel estimation is concerned. On the contrary, they may have a different impact on the system spectral efficiency, depending on the type of linear receiver considered. Therefore, it is interesting to study system spectral efficiency with pilot symbols or pilot signals for leaving ε as a parameter, where ε is designed in order to achieve (almost) perfect coherent detection.

Asymptotic SINR with Pilot Symbols: With this scheme, a fraction ε of the transmitted symbols are pilot symbols known to the receiver. The symbol rate necessary to achieve bit rate R_b is $R_s = R_b/((1 - \varepsilon)R)$, where R is the channel coding rate, expressed in bits/symbol. The resulting spreading gain is given by $L = W/R_s = (1-\varepsilon)RW/R_b$ chip/symbol, where for simplicity we assume that the chip rate is equal to the system bandwidth W,[2] and that L is an integer.

The SNR for each user is given by $\gamma = (\mathcal{P}/R_s)/N_0 = (1 - \varepsilon)RE_b/N_0$, and the channel load is given by $\alpha = K/L = \eta/((1-\varepsilon)R)$. By using these expressions in (3) and by using the fact that all users have the same SNR (i.e., $\gamma_I = \gamma$ with probability 1), we obtain the asymptotic output SINR as a function of the basic system parameters

$$\beta = \begin{cases} \dfrac{(1-\varepsilon)RE_b/N_0}{1 + \eta E_b/N_0} & \text{(SUMF)} \\ \dfrac{(1-\varepsilon)RE_b/N_0}{1 + \eta \dfrac{E_b/N_0}{1 + \beta}} & \text{(LMMSE)}. \end{cases} \qquad (4)$$

---

[2]This is equivalent to assume ideal zero excess-bandwidth Nyquist chip-shaping pulses. In UMTS, the chip-shaping pulse is root-raised cosine [20] with rolloff 0.22 (see [12] and references therein).

Asymptotic SINR with Pilot Signals: With this scheme, each user transmits a data signal at power $(1 - \epsilon)\mathcal{P}$ and a pilot signal at power $\epsilon\mathcal{P}$. Pilot signals are spread-spectrum signals, formally identical to data signals, but modulated by a training symbol sequence known to the receiver. The system with pilot signals is equivalent to a system with $2K$ virtual users. "Data" and "pilot" users have the same symbol rate $R_s = R_b/R$ and SNRs $\gamma_1 = (1 - \epsilon)PRE_b/N_0$ and $\gamma_2 = \epsilon RE_b/N_0$, respectively. By using these expressions in (3) and by using the fact that there are K virtual users with SNR γ_1 and K virtual users with SNR γ_2 (i.e., γ_I takes on values γ_1 and γ_2 with probability $1/2$), we obtain the asymptotic output SINR as a function of the basic system parameters

$$\beta =
\begin{cases}
\dfrac{(1-\epsilon)RE_b/N_0}{1+\eta E_b/N_0}, & \text{(SUMF)} \\[2ex]
\dfrac{(1-\epsilon)RE_b/N_0}{1+(1-\epsilon)\eta E_b/N_0\left(\dfrac{1}{1+\beta} + \dfrac{\epsilon}{1-\epsilon+\epsilon\beta}\right)}, & \text{(LMMSE).}
\end{cases}$$

(5)

Notice that, with the SUMF receiver, pilot signals and pilot symbols yield the same asymptotic SINR. Therefore, these techniques with SUMF are equivalent in terms of system spectral efficiency.

QoS Constraints: The user coding rate R is related to the desired SINR β at the receiver output by some QoS requirement. Typically, the function $R = R(\beta)$ for any meaningful QoS constraint is nondecreasing in β. Depending on the application, QoS is given in terms of the target bit-error rate (BER) or frame-error rate (FER). For example, data transmission requires very small FER (e.g., $\leq 10^{-6}$) and speech transmission (mobile telephony) requires not too large BER (e.g., between 10^{-2} and 10^{-3}). Driven by this rationale, we consider an FER constraint suited to data transmission and a BER constraint suited to speech transmission. In particular, we study the asymptotic system spectral efficiency subject to the following.

1) Arbitrarily small FER, assuming optimal channel codes (i.e., single-user capacity achieving Gaussian codes). Since with Gaussian codes the output of the receiver linear filter is Gaussian, this yields the rate function $R(\beta) = \log_2(1 + \beta)$, where β is the SINR at the receiver filter output.

2) Given target BER, assuming uncoded quadrature amplitude modulation (QAM)/phase-shift keying (PSK) modulation with m bits/symbol. This yields the rate function

$$R(\beta) = m, \qquad \text{for } \beta_m \leq \beta < \beta_{m+1}$$

(6)

where β_m is defined as the minimum required SINR for which a QAM/PSK modulation with cardinality 2^m achieves the target BER (with coherent detection).

We evaluate the BER as a function of β by making a Gaussian approximation of the receiver filter output and by assuming Gray binary labeling of the modulation symbols [20]. Then, the BER of QAM/PSK modulations is given by

$$\text{BER} \approx
\begin{cases}
Q(\sqrt{2\beta}), & m = 1 \quad \text{(BPSK)} \\[1ex]
Q(\sqrt{\beta}), & m = 2 \quad \text{(QPSK)} \\[1ex]
\dfrac{2}{m}Q\left(\sqrt{2\sin^2\left(\dfrac{\pi}{2^m}\right)\beta}\right), & m = 3 \quad \text{(8PSK)} \\[2ex]
\dfrac{4}{m}Q\left(\sqrt{\dfrac{3\beta}{2^m - 1}}\right), & m > 3 \quad (2^m\text{-QAM}).
\end{cases}$$

(7)

where $Q(x) \triangleq (2\pi)^{-1/2} \int_x^\infty \exp(-u^2/2) \, du$.

A. Spectral Efficiency with the FER Constraint

We study the system spectral efficiency η as a function of the required SINR β for the coding rate $R(\beta) = \log_2(1 + \beta)$ induced by the above FER constraint, and by treating E_b/N_0 and ϵ as given system parameters.

The asymptotic SINR equations (4) and (5) can be put in the form

$$\beta = \frac{(1 - \varepsilon)R(\beta)\,E_b/N_0}{1 + \zeta(\beta)\,\eta\,E_b/N_0}$$

(8)

where $R(\beta) = \log_2(1+\beta)$ and given in (9), shown at the bottom of the page. Following the approach of [4, Proposition 3.2], we rewrite (8) as

$$g(\beta) \triangleq \frac{\beta(1 + \zeta(\beta)\,\eta\,E_b/N_0)}{(1 - \varepsilon)R(\beta)\,E_b/N_0}.$$

(10)

We notice that

$$\lim_{\beta \to 0} g(\beta) = \frac{(1 + \eta\,E_b/N_0)}{(1 - \varepsilon)\,E_b/N_0}\log(2)$$

for all types of receivers considered. The function $g(\beta)$ is strictly increasing for $\beta > 0$ with the SUMF while it first decreases to a minimum and then increases with the LMMSE.

As far as the solution of (10) with respect to β is concerned, the following remarks are in order.

- The solution of (10) may not exist or may not be unique. In fact, this behavior of the SINR equation is different from

$$\zeta(\beta) =
\begin{cases}
\zeta_{\text{SUMF}}(\beta) = 1, & \text{(Pilot symbols or pilot signals, SUMF)} \\[1ex]
\zeta_{\text{MMSE},1}(\beta) = \dfrac{1-\varepsilon}{1+\beta} + \dfrac{\varepsilon}{1+(\varepsilon/(1-\varepsilon))\beta}, & \text{(Pilot signals, LMMSE)} \\[1ex]
\zeta_{\text{MMSE},2}(\beta) = 1/(1+\beta), & \text{(Pilot symbols, LMMSE)}
\end{cases}$$

(9)

the case of [4, Proposition 3.2], where γ is assumed to be independent of the coding rate.

- If $\eta < (1 - \varepsilon) \log_2 e - 1/(E_b/N_0)$, (10) has a unique solution which satisfies the inequalities

$$\beta_{\text{SUMF}} < \beta_{\text{MMSE},1} < \beta_{\text{MMSE},2}$$

deriving from

$$\zeta_{\text{SUMF}}(\beta) > \zeta_{\text{MMSE},1}(\beta) > \zeta_{\text{MMSE},2}(\beta) \qquad (11)$$

which holds under the reasonable assumption that $\varepsilon \leq 0.5$ (i.e., less than 50% of the system resources are devoted to pilot transmission).

- Otherwise, there is no solution for the SUMF, but there may be one for the LMMSE with pilot symbols or pilot signals. In both cases, if any solution exists, there are two ones, and the smaller must be discarded. A solution exists if and only if the minimum of $g(\beta)$ for $\beta > 0$ is smaller than 1.

By solving (10), we obtain β as a function of η and the system parameters E_b/N_0 and ϵ. Equivalently, from (8), we can write the system spectral efficiency η as a function of β

$$\eta(\beta) = \frac{1}{\zeta(\beta)} \left[\frac{(1 - \varepsilon) R(\beta)}{\beta} - \frac{1}{E_b/N_0} \right]_+. \qquad (12)$$

The following remarks are in order.

- The E_b/N_0 necessary to have nonzero spectral efficiency for given β and ε must satisfy

$$\frac{E_b}{N_0} \geq \left(\frac{E_b}{N_0} \right)_{\min} \triangleq \frac{\beta}{(1 - \varepsilon) R(\beta)}.$$

- By using (11) into (12), still assuming that less than 50% of the system resources are devoted to pilot transmission, the system spectral efficiencies with the different types of receiver are ordered as follows:

$$\eta_{\text{SUMF}}(\beta) < \eta_{\text{MMSE},1}(\beta) < \eta_{\text{MMSE},2}(\beta).$$

Intuitively, the performance of the LMMSE receiver with pilot signals is worse than with pilot symbols because the former case is equivalent to having $2K$ users and spreading gain $L = RW/R_b$, while the latter is equivalent to having only K users and spreading gain reduced by the factor $(1 - \epsilon)$. For $\epsilon < 0.5$, the channel load (total number of equivalent users per chip) is larger in the pilot signals case. In other words, pilot signals expand the dimension of the signal subspace spanned by the multiple-access interference. Now, it is well known that linear multiuser receivers perform poorly when the dimension of the interference subspace is a large fraction of the spreading gain [7] (this effect is sometimes referred to as "dimensional crowding" [22]). For $\epsilon = 0.5$, the two system have the same spectral efficiency, as can be seen by inspection of (4) and (5).

Figs. 1 and 2 show η versus β for $E_b/N_0 = 2$ and 10 dB, and for $\varepsilon = 0.2$. This corresponds to about -6 dB of pilot-to-data signal power ratio and to one pilot every five transmitted symbols. These values appear to be quite realistic in order to ensure coherent detection, as shown by simulations of practical systems [15], [14].
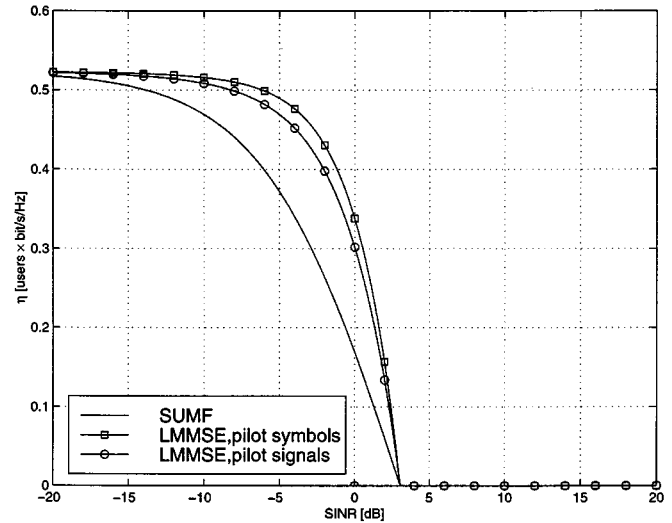

Fig. 1. Asymptotic spectral efficiency η of DS-CDMA versus required SINR β with $\epsilon = 0.20$ and $E_b/N_0 = 2$ dB.
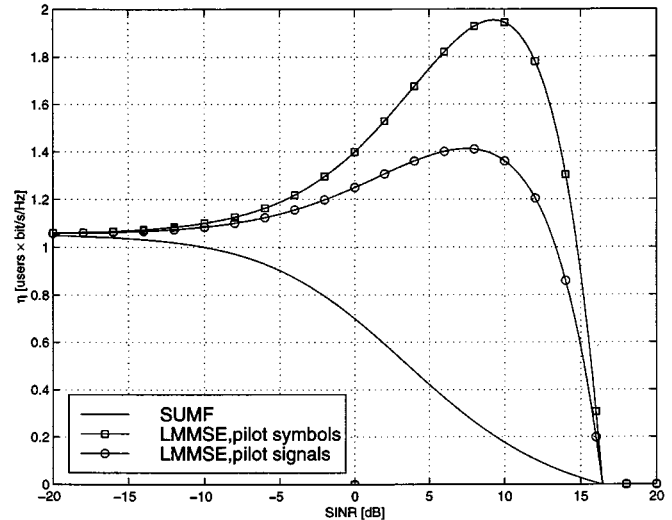

Fig. 2. Asymptotic spectral efficiency η of DS-CDMA versus required SINR β with $\epsilon = 0.20$ and $E_b/N_0 = 10$ dB.

Qualitatively, we observe that, for low values of E_b/N_0 (see Fig. 1), the asymptotic system spectral efficiency for both the SUMF and the LMMSE receivers decreases as the target SINR β increases. The system spectral efficiency is maximized by $\beta \to 0$, which implies $R \to 0$. From a practical system design point of view, this means that, for low E_b/N_0, a system optimized for spectral efficiency has a very large number of users with negligible coding rate. The overall bandwidth expansion factor W/R_b is entirely devoted to low-rate coding and the spreading gain should be as small as possible (i.e., $L = 1$). This kind of systems is proposed, for example, in [21] under the name of *code-spread CDMA*.

On the contrary, with LMMSE and sufficiently high E_b/N_0 (see Fig. 2), η is first increasing and then decreasing with β. From a practical system design point of view, this means that in a system optimized for spectral efficiency the overall bandwidth expansion factor W/R_b is allocated partly to spreading and partly to coding. The optimum coding rate

is $R_{\mathrm{opt}} = \log_2(1 + \beta_{\mathrm{opt}})$ and the corresponding optimum spreading gain is given by

$$L = R(\beta_{\mathrm{opt}})\frac{W}{R_b} \tag{13}$$

where β_{opt} is the value of the target SINR maximizing η.

In all cases, η approaches zero for $\beta \geq \beta_{\max}(\epsilon, E_b/N_0)$ which is a solution of the equation

$$\frac{\beta}{\log_2(1 + \beta)} = (1 - \varepsilon)\frac{E_b}{N_0}. \tag{14}$$

Interestingly, $\beta_{\max}(\epsilon, E_b/N_0)$ depends on ε and on E_b/N_0, and it is independent of the type of receiver and of the pilot technique.

We can prove analytically the above qualitative results by considering the expression (12) of the system spectral efficiency. We obtain the following.

- For the SUMF

$$\frac{d}{d\beta}\eta(\beta) = (1 - \varepsilon)\left[-\frac{\log_2(1+\beta)}{\beta^2} + \frac{\log_2 e}{(\beta+1)\beta}\right] < 0$$

  for $\varepsilon \in (0, 1)$ and $\beta > 0$, which implies that η is a decreasing function of β.

- For the LMMSE with pilot symbols

$$\frac{d^2}{d\beta^2}\eta(\beta) = (1 - \varepsilon)\left[2\frac{\log_2(1+\beta)}{\beta^3} - \frac{(\beta+2)\log_2 e}{(\beta+1)\beta^2}\right] < 0.$$

  Hence, there may be a single zero of $(d/d\beta)\eta(\beta)$ (and a maximum of $\eta(\beta)$) provided that $(d/d\beta)\eta(0) > 0$, which holds if and only if

$$\frac{E_b}{N_0} > \left(\frac{E_b}{N_0}\right)_{\mathrm{th}} = \frac{2\log 2}{1 - \varepsilon}. \tag{15}$$

- With pilot signals, the analysis is more complicated. However, we can show that $\eta(\beta)$ has a maximum for positive β for $\varepsilon < 0.5$ and all E_b/N_0 above the value

$$\left(\frac{E_b}{N_0}\right)_{\mathrm{th}} = \frac{2\log 2}{1 - \varepsilon}\left[1 + \frac{\varepsilon(1 - 2\varepsilon)}{1 - 3\varepsilon + 4\varepsilon^2}\right] > \frac{2\log 2}{1 - \varepsilon}. \tag{16}$$

In other words, with the LMMSE receiver, there exists a threshold value of E_b/N_0, albeit quite low, below which the system spectral efficiency is maximized by $\beta \to 0$, and coincides with the maximum spectral efficiency attained by the SUMF. In this case, if system spectral efficiency is the main performance indicator, there is no point in using the more complicated LMMSE receiver. By letting $\varepsilon = 0.2$ in (15), we obtain the threshold value $(E_b/N_0)_{\mathrm{th}} = 2.39$ dB, which is in agreement with the behavior shown in Figs. 1 and 2.

B. Spectral Efficiency with Uncoded QAM and BER Constraint

Consider now the case of uncoded QAM, for which $R(\beta)$ is given by (6). The closed-form analysis in this case is complicated by the fact that $R(\beta)$ is a piecewise constant function of β. However, the behavior of $\eta(\beta)$ is qualitatively similar to that observed above for the case of optimal Gaussian codes.

Figs. 3 and 4 show the system spectral efficiency for target BER equal to $10^{-2}, \varepsilon = 0.2, E_b/N_0 = 10$ and 15 dB, re-
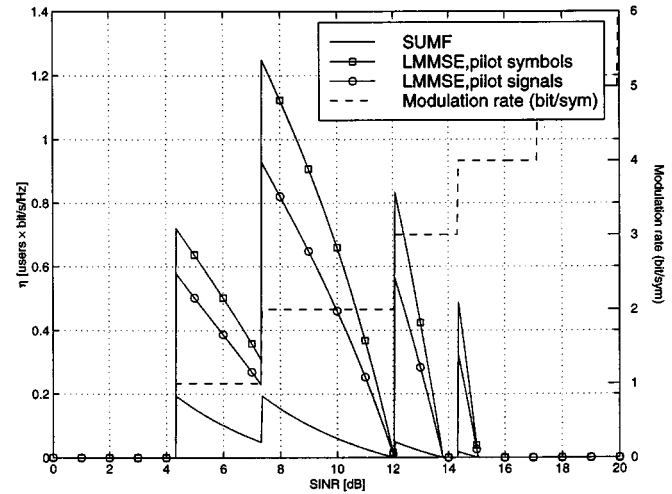

Fig. 3. Asymptotic spectral efficiency η of DS-CDMA versus required SINR β with $\epsilon = 0.20$, $E_b/N_0 = 10$ dB, and uncoded QAM/PSK with target BER equal to 10^{-2}.
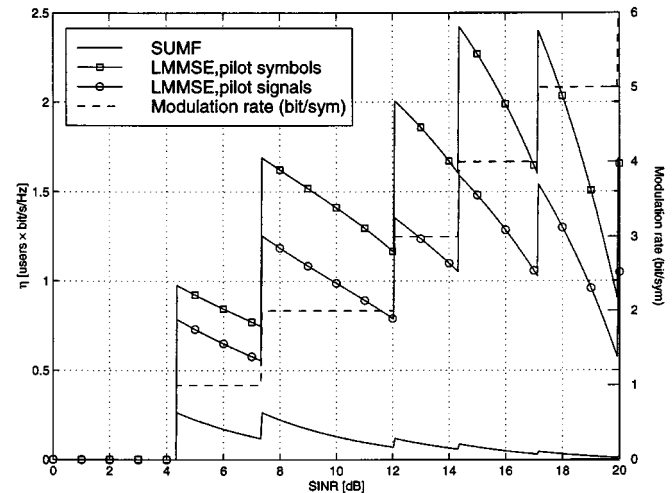

Fig. 4. Asymptotic spectral efficiency η of DS-CDMA versus required SINR β with $\epsilon = 0.20$, $E_b/N_0 = 15$ dB, and uncoded QAM/PSK with target BER equal to 10^{-2}.

spectively. The peaks of the spectral efficiency curves correspond (from left to right) to binary PSK (BPSK), quadrature PSK (QPSK), 8PSK, 16QAM, and 32QAM constellations.

With the SUMF, the maximum spectral efficiency is attained by BPSK and QPSK. It is easy to show that these two modulation formats are equivalent in terms of spectral efficiency, since the BPSK system is able to support twice as many users as the QPSK system, with half bits/second/Hertz per user.

With the LMMSE receiver, a different behavior can be observed. For E_b/N_0 lower than a threshold, the spectral efficiency is maximum for QPSK (see Fig. 3). We notice that QPSK and BPSK are not equivalent with LMMSE detection. In particular, it can be shown that QPSK yields better spectral efficiency than BPSK for all E_b/N_0. This is due to the dimensional crowding effect already observed for pilot signals, since the BPSK would need to support twice as many users as the QPSK system, in order to have the same spectral efficiency. For E_b/N_0 larger than the threshold, the spectral efficiency is maximum for signal constellations larger than QPSK (see Fig. 4, where

the maximum is attained by 16QAM). The threshold value of E_b/N_0 can be calculated numerically, and depends on the BER target and on ε.

IV. COMPARISON OF MULTIRATE FORMATS

In this section, we show how the asymptotic random sequence analysis can be used to select a multirate format. We consider two user classes of size K_1 and K_2, with bit rates $R_{b1} < R_{b2}$ bits/s, respectively, and assume that the rate ratio $r = R_{b2}/R_{b1}$ is an integer greater than 1.

As before, we study the asymptotic system performance in the limit for $K_1, K_2 \to \infty$, while the numbers of users per chip K_1/L and K_2/L converge to constant values α_1 and α_2, respectively. Let β_i and γ_i be the SINR at the linear receiver output (SUMF or LMMSE) and the SNR of a user in class $i = 1, 2$. The two classes are characterized by SINR requirement $\beta_i \geq \bar{\beta}_i$ and SNR constraint $\gamma_i \leq \bar{\gamma}_i$. Following [4], we define the multirate system capacity region $\mathcal{R}$ as

$$\mathcal{R} = \{(\alpha_1, \alpha_2) \in \mathbb{R}_+^2; \beta_i \geq \bar{\beta}_i, \gamma_i \leq \bar{\gamma}_i, \quad \text{for } i = 1, 2\}. \tag{17}$$

The boundary of $\mathcal{R}$ is the set of pairs (α_1, α_2) for which it is not possible to stay in $\mathcal{R}$ by increasing both components.

Among the methods recently proposed for implementing multirate CDMA (see, e.g., [16]–[19]), we examine and compare multimodulation (MM), multicode (MC), and variable spreading (VS).

A. Multimodulation Scheme

With MM, users of both classes transmit with the same symbol rate R_s, by using different coded-modulation schemes with spectral efficiency $R_1 = R_{b1}/R_s$ and $R_2 = R_{b2}/R_s$ bits/symbol, respectively. The spreading gain $L = W/R_s$ is common to both classes.

Since the two sets of users transmit with different coded-modulation schemes, they have different SINR requirements $\bar{\beta}_1$ and $\bar{\beta}_2$. In order to obtain results independent of the specific coded-modulation schemes used, we assume that optimal Gaussian codes are used. Thus, the SINR requirements are

$$\begin{aligned} \bar{\beta}_1 &= 2^{R_1} - 1 \\ \bar{\beta}_2 &= 2^{R_2} - 1. \end{aligned} \tag{18}$$

The asymptotic capacity region for MM has been found in [4]. For the sake of completeness, we provide the expression in the case of two classes considered in this paper. With SUMF receiver, $\mathcal{R}$ is defined by the inequality

$$\alpha_1 \bar{\beta}_1 + \alpha_2 \bar{\beta}_2 \leq \min \left\{ \left[1 - \frac{\bar{\beta}_1}{\bar{\gamma}_1}\right]_+, \left[1 - \frac{\bar{\beta}_2}{\bar{\gamma}_2}\right]_+ \right\}. \tag{19}$$

With LMMSE receiver, $\mathcal{R}$ is defined by the inequality

$$\alpha_1 \frac{\bar{\beta}_1}{1 + \bar{\beta}_1} + \alpha_2 \frac{\bar{\beta}_2}{1 + \bar{\beta}_2} \leq \min \left\{ \left[1 - \frac{\bar{\beta}_1}{\bar{\gamma}_1}\right]_+, \left[1 - \frac{\bar{\beta}_2}{\bar{\gamma}_2}\right]_+ \right\}. \tag{20}$$

(Obviously, this includes the SUMF asymptotic capacity region.)

An interesting property of MM is that the optimal power allocation problem can be solved in closed form. In fact, for all $(\alpha_1, \alpha_2) \in \mathcal{R}$, the SNRs γ_i required to achieve SINRs $\bar{\beta}_i$ is given by

$$\gamma_i = \begin{cases} \dfrac{\bar{\beta}_i}{1 - \sum_{j=1}^2 \alpha_j \bar{\beta}_j} & \text{(SUMF)} \\[4mm] \dfrac{\bar{\beta}_i}{1 - \sum_{j=1}^2 \alpha_j \frac{\bar{\beta}_j}{1+\bar{\beta}_j}} & \text{(LMMSE).} \end{cases} \tag{21}$$

We can make here a link to the results of [23], which will be useful in the discussion of the VS case below. In [23], it is shown that most power control problems can be formulated in the form $\gamma \geq \mathbf{I}(\gamma)$, where γ is the vector of assigned user SNRs, and $\mathbf{I}(\gamma) = (I_1(\gamma), \ldots, I_K(\gamma))$ is a (vector) interference function. An interference function is said to be *feasible* if there exists a nonnegative solution γ to the above inequality. The interference function $\mathbf{I}(\gamma)$ is said to be *standard* if the following conditions hold for all $\gamma > \mathbf{0}$: a) $\mathbf{I}(\gamma) > \mathbf{0}$ (positivity); b) $\gamma \geq \gamma' \Rightarrow \mathbf{I}(\gamma) \geq \mathbf{I}(\gamma')$ (monotonicity); and c) $\kappa \mathbf{I}(\gamma) > \mathbf{I}(\kappa\gamma)$ for all $\kappa > 1$ (scalability). If $\mathbf{I}(\gamma)$ is standard, the power control iteration

$$\gamma_{n+1} = \mathbf{I}(\gamma_n) \tag{22}$$

is globally convergent to a unique SNR vector γ^*. Moreover, γ^* the componentwise minimum feasible SNR assignment, i.e., for every γ achieving the SINR target for all users, $\gamma \geq \gamma^*$ [23].

In our case, the required SINR targets $\bar{\beta}_i$ are met by both classes if [4]

$$\bar{\beta}_i \leq \begin{cases} \dfrac{\gamma_i}{1 + \sum_{j=1}^2 \alpha_j \gamma_j} & \text{(SUMF)} \\[4mm] \dfrac{\gamma_i}{1 + \sum_{j=1}^2 \alpha_j \frac{\gamma_j \gamma_i}{\gamma_i + \gamma_j \bar{\beta}_i}} & \text{(MMSE).} \end{cases} \tag{23}$$

The above inequalities yield the interference function defined componentwise (for $i = 1, 2$) by

$$I_i(\gamma_1, \gamma_2) = \begin{cases} \bar{\beta}_i \left(1 + \sum_{j=1}^2 \alpha_j \gamma_j\right) & \text{(SUMF)} \\[4mm] \bar{\beta}_i \left(1 + \sum_{j=1}^2 \alpha_j \frac{\gamma_j \gamma_i}{\gamma_i + \gamma_j \bar{\beta}_i}\right) & \text{(LMMSE).} \end{cases}$$

It is easy to show that the above interference function is standard and that the SNR assignment given by (21) is the unique fixed point of iteration (22), i.e., it is the componentwise minimum feasible SNR assignment.

The boundary of $\mathcal{R}$ is given by equality in (19) [respectively, in (20)]. In general, the minimum in the right-hand side (RHS) is achieved by one of the classes (say, class i). Then, the power control solution (21) gives $\gamma_i = \bar{\gamma}_i$ for class i, while $\gamma_j < \bar{\gamma}_j$ for the other class. In other words, the users in the class with the tightest power constraint must transmit at their maximum SNR, while the users in the class with loosest power constraint transmit at SNR below their maximum. The system capacity is limited by the class with largest ratio $\bar{\beta}_i/\bar{\gamma}_i$.

B. Multicode Scheme

With MC, every high-rate user divides its data stream into r substreams ("virtual low-rate users"). Each substream is individually spread and transmitted, and each virtual user is detected by an independent receiver. Under the assumption of random spreading, the MC system is equivalent to a single-rate system with $\alpha = \alpha_1 + r\alpha_2$ users/chip, all with the same bit-rate R_{b1}, or, equivalently, with the same spectral efficiency $R_1 = TR_{b1}$. The SINR requirement is $\bar{\beta}_1$ given in (18) and the capacity region is immediately obtained as

$$\alpha_1 + r\alpha_2 \leq \begin{cases} \left[\frac{1}{\bar{\beta}_1} - \frac{1}{\bar{\gamma}_1}\right]_+ & \text{(SUMF)} \\ (1 + \bar{\beta}_1)\left[\frac{1}{\bar{\beta}_1} - \frac{1}{\bar{\gamma}_1}\right]_+ & \text{(LMMSE)} \end{cases} \tag{24}$$

where $\bar{\gamma}_1$ is the SNR constraint for a user of the equivalent single-rate system.

The boundary of the MC capacity region is achieved when each equivalent low-rate user transmits at its maximum SNR $\bar{\gamma}_1$. This implies that the transmit power of high-rate users is equal to r times the transmit power of low-rate users, as it is obvious from the signal-splitting MC approach.

Also, we must keep in mind that the capacity regions derived by the asymptotic analysis are valid for random spreading sequences. With MC, all the r virtual users corresponding to the same high-rate user could be made orthogonal by choosing mutually orthogonal spreading sequences (typically, different Walsh–Hadamard sequences, chip-wise multiplied by a common scrambling sequence in order to randomize nonorthogonal interference from the other users). The random-signature sequence approach followed in this paper cannot take this orthogonality constraint into consideration. However, mutual orthogonality is expected to have little impact on the uplink, since the main source of impairment is the nonorthogonal interference from other users.

C. Variable-Spreading Scheme

With VS, high-rate users transmit with a symbol rate rR_s. Thus, the effective spreading sequence length for a high-rate user is L/r (assumed to be integer). This is conceptually similar to the multicode scheme: in fact, a high-rate user can be decomposed into r virtual low-rate users whose sequences are zero in a part of the "long" symbol interval, as shown in Fig. 5. Both classes of users have the same coded-modulation spectral efficiency R_1. In fact, $R_1 = R_{b1}/R_s = R_{b2}/(rR_s)$, since $R_{b2} = rR_{b1}$. High-rate users transmit at power r times larger than low-rate users. Since their symbol rate is r times larger, their SNR constraint (energy per symbol over N_0) is the same as for low-rate users. Hence, as in the MC case, all users have the same SINR requirement $\bar{\beta}_1 = 2^{R_1} - 1$ and the same SNR constraint $\bar{\gamma}_1$.

Intuitively, we expect that the capacity region of VS is somewhat similar to that of MC. However, the asymptotic analysis based on purely random sequences is not directly applicable in this case, because the spreading sequences, being constrained to be zero on certain symbols, are not random. Nevertheless,
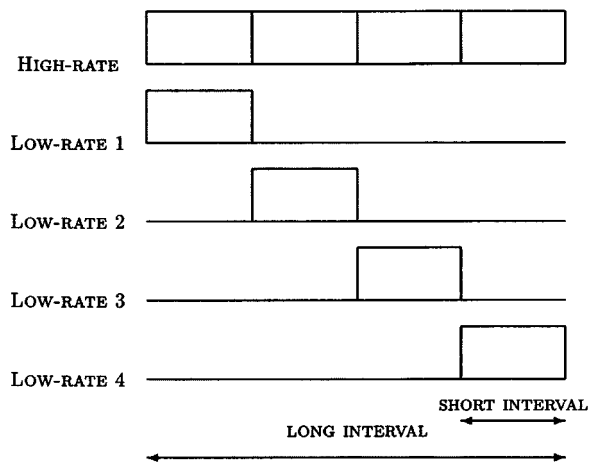

Fig. 5. Decomposition of a high-rate user into r low-rate virtual users ($r = 4$ in this example).

by applying the powerful results of [6] (used in [8] to solve the single-rate chip-synchronous symbol-asynchronous CDMA case), we obtain closed-form results also for VS. These results (which are new to the authors' knowledge) are stated in the following propositions whose proof is postponed to Appendix A.

Proposition 1: With the SUMF receiver, the asymptotic system capacity region of VS is exactly the same of MC, given in (24). □

Now, we turn our attention to the more interesting case of LMMSE receiver. For low-rate users, we have the following.

Proposition 2: With the LMMSE, the asymptotic SINR of **low-rate** users is given by the unique nonnegative solution of the fixed-point equation

$$\beta_1 = \frac{\gamma_1}{1 + \alpha_1 \frac{\gamma_1}{1 + \beta_1} + r\alpha_2 \frac{\gamma_1\gamma_2}{\gamma_1 + \beta_1\gamma_2}}. \tag{25}$$

□

With the LMMSE, the symbols of high-rate users can be detected either by considering only the short symbol interval of duration $1/(rR_s)$ over which the corresponding spreading sequence is nonzero, or by considering the whole symbol interval of duration $1/R_s$ [16]. For the sake of brevity, we nickname these two linear detection schemes for high-rate users as "short-interval" and "long-interval," respectively. Short-interval detection is less complex, since it requires shorter linear filters. However, since the interference created by low-rate user symbols over high-rate user symbols is correlated over the whole long symbol interval, we expect that the short-interval detection suffers from some performance degradation. We have the following.

Proposition 3: With LMMSE receiver and **short-interval** detection, the asymptotic SINR of **high-rate** users is the unique nonnegative solution of the fixed-point equation

$$\beta_2 = \frac{\gamma_2}{1 + \alpha_1 \frac{\gamma_1\gamma_2}{\gamma_2 + \gamma_1\beta_2/r} + r\alpha_2 \frac{\gamma_2}{1 + \beta_2}}. \tag{26}$$

□

Proposition 4: With LMMSE receiver and **long-interval** detection, the asymptotic SINR of **high-rate** users is given by the unique nonnegative solution of the fixed-point equation

$$\beta_2 = \frac{\gamma_2}{1 + \alpha_1 \dfrac{\gamma_1 \gamma_2}{\gamma_2(1+\hat{\beta}) + \gamma_1 \beta_2/r} + r\alpha_2 \dfrac{\gamma_2}{1+\beta_2}} \quad (27)$$

where $\hat{\beta}$ is the unique nonnegative solution of the fixed-point equation

$$\hat{\beta} = \frac{\dfrac{r-1}{r}\gamma_1}{1 + \alpha_1 \dfrac{\gamma_1}{1+\hat{\beta}} + r\alpha_2 \dfrac{\gamma_1\gamma_2}{\gamma_1 + \hat{\beta}\frac{r}{r-1}}} \quad (28)$$

□

The following result states the desired comparison between MC and VS.

Proposition 5: Let $\mathcal{R}^{\mathrm{MC}}, \mathcal{R}^{\mathrm{VS,long}}$, and $\mathcal{R}^{\mathrm{VS,short}}$ denote the capacity regions with LMMSE receiver for the MC, VS (long-interval detection), and VS (short-interval detection) systems. Then, the inclusion relation

$$\mathcal{R}^{\mathrm{MC}} \supseteq \mathcal{R}^{\mathrm{VS,long}} \supseteq \mathcal{R}^{\mathrm{VS,short}}$$

holds for all given system parameters (SINR requirement $\bar{\beta}_1$, rate ratio $r > 1$, and SNR constraint $\bar{\gamma}_1$). □

Unfortunately, the power control problem for VS with LMMSE receiver does not have a nice closed-form solution as for MM. Then, in order to plot the capacity region boundary for VS/LMMSE, we resort to a semi-analytic method exploiting the power control iteration (22) with the proper definition of a standard interference function.

By substituting $\beta_1 = \beta_2 = \bar{\beta}_1$ into the SINR equations (25)–(27), we obtain the interference function (defined componentwise)

$$I_1(\gamma_1, \gamma_2) = \bar{\beta}_1 \left(1 + \alpha_1 \frac{\gamma_1}{1+\bar{\beta}_1} + r\alpha_2 \frac{\gamma_1\gamma_2}{\gamma_1 + \bar{\beta}_1\gamma_2} \right)$$

$$I_2(\gamma_1, \gamma_2) = \bar{\beta}_1 \left(1 + \alpha_1 \frac{\gamma_1\gamma_2}{\gamma_2(1 + y(\gamma_1,\gamma_2)) + \gamma_1\bar{\beta}_1/r} \right.$$
$$\left. + r\alpha_2 \frac{\gamma_2}{1+\bar{\beta}_1} \right) \quad (29)$$

where $y(\gamma_1, \gamma_2) = 0$ for short-interval detection and $y(\gamma_1, \gamma_2) = \hat{\beta}$ for long-interval detection. The above interference function is standard.

From [23], we know that the new interference function including the SNR constraint, given by

$$I_i^{\mathrm{constr.}}(\gamma_1, \gamma_2) = \min\{I_i(\gamma_1, \gamma_2), \bar{\gamma}_1\}$$

is also standard. Therefore, the resulting power control recursion (22) is globally convergent. Moreover, its unique fixed point γ^* has the property that if

$$\gamma_i^* = I_i(\gamma^*) \leq \bar{\gamma}_1 \quad (30)$$

then the SINR requirement for class i is satisfied, while if

$$\gamma_i^* = \bar{\gamma}_1 < I_i(\gamma^*) \quad (31)$$

then the SINR requirement for class i is not satisfied. In order to check if a pair (α_1, α_2) is inside the capacity region, it is sufficient to run the power control recursion based on $\mathbf{I}^{\mathrm{constr.}}(\gamma)$ and calculate its fixed point γ^*. If (30) is met for both $i = 1, 2$, then $(\alpha_1, \alpha_2) \in \mathcal{R}$.

Since the interference function is componentwise increasing in α_1 and α_2, it is easy to see that any straight line $\alpha_2 = z\alpha_1$, for $z \in \mathbb{R}_+$, intersects the capacity region boundary in a single point. Then, the points on the boundary can be obtained by searching for the intersection for all directions z.[3]

D. Numerical Results

In our example, low-rate users transmit with spectral efficiency $R_1 = 0.5$ bits/symbol and the rate ratio is $r = 4$ (i.e., $R_{b1} = 0.5R_s$ and $R_{b2} = 2R_s$ bits/s, where R_s is the symbol rate of low-rate users). We compare the system capacity assuming that both low-rate and high-rate users have the same E_b/N_0. Then, the SNR constraint for low-rate users (in MM) and for both low-rate and equivalent low-rate users (in MC and VS) is given by $\bar{\gamma}_1 = R_1 E_b/N_0$, while the SNR constraint for high-rate users in MM is given by $\bar{\gamma}_2 = rR_1 E_b/N_0 = r\bar{\gamma}_1$.

Figs. 6 and 7 show the asymptotic capacity region boundaries for MM, MC, and VS with SUMF and LMMSE receivers, for $E_b/N_0 = 3$ dB and $E_b/N_0 = 10$ dB, respectively. Some comments are in order.

1) Equivalence of MC and VS (Long-Interval Detection): The capacity regions of MC and VS with LMMSE and long-interval detection are almost identical. In Appendix A, we prove that the term $\hat{\beta}$ in Proposition 4 satisfies

$$\hat{\beta} \leq \frac{r-1}{r}\beta_1$$

where β_1 is the solution of (25), i.e., it is the SINR of low-rate users in the VS system. If we replace $\hat{\beta}$ by $(r - 1/r)\beta_1$ in (27), it is immediate to show that the optimal power control yields $\gamma_1 = \gamma_2 = \bar{\gamma}_1$, which implies $\beta_1 = \beta_2$. With this substitution, the expressions of β_1 and β_2 become identical to that of β_1 in the MC system, therefore the corresponding capacity region coincides with that of MC. From the above argument, it is intuitive to see that if $\hat{\beta}$ is very close to $(r - 1/r)\beta_1$, then the VS and the MC capacity regions will be also very close. This is precisely what happens for our choice of system parameters. Most importantly, we checked numerically that this fact occurs for a very wide range of system parameters ($E_b/N_0, R_1$ and r). Therefore, we can conclude that the MC and the VS (with long-interval detection) systems are (almost) equivalent from the asymptotic capacity point of view.

2) Comparison Between MM and MC: In Appendix B, we prove that, with LMMSE receiver, the (absolute) slope of the MM capacity region boundary is always larger than that of MC,

[3]Notice that, unlike the capacity region of the "classical" multiple-access channel [24], these capacity regions need not be convex, unless an explicit convexification based on time-sharing between different pairs (α_1, α_2) is done (this is equivalent to take the convex hull of the points obtained from the above algorithm).
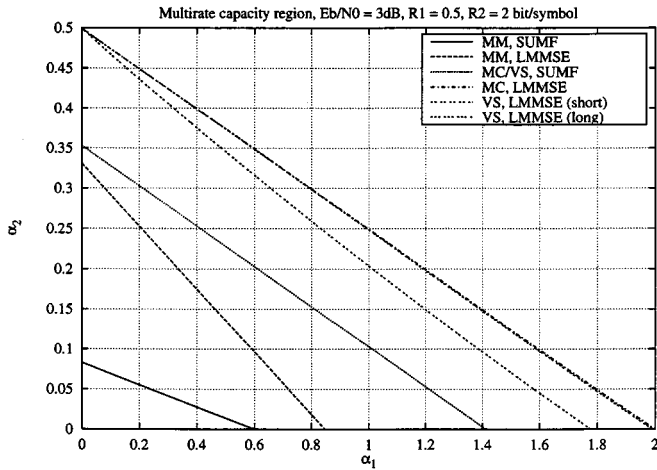
Fig. 6. Capacity regions of MM, MC, and VS systems, for $R_1 = 0.5$ bit/symbol, $r = 4$, and $E_b/N_0 = 3$ dB.
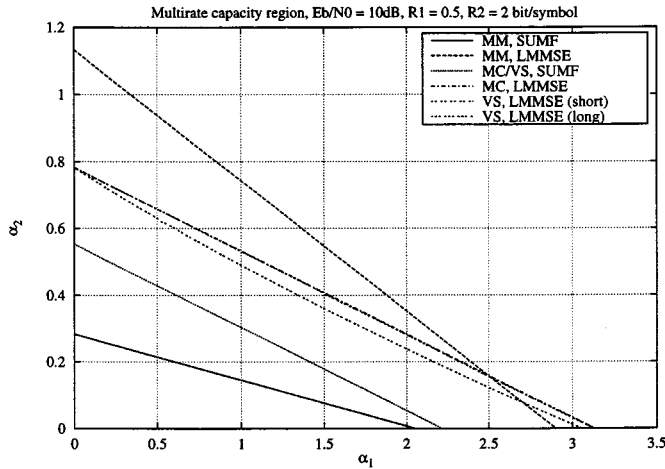

Fig. 7. Capacity regions of MM, MC, and VS systems, for $R_1 = 0.5$ bit/symbol, $r = 4$, and $E_b/N_0 = 10$ dB.

that the MM capacity region boundary intersects the horizontal axis in α_1 always less than the corresponding intersection of MC, and that an intersection of the two boundaries exists if

$$E_b/N_0 \geq \frac{1}{R_1} \frac{\left(1 - 2^{(1-r)R_1}\right)\left(2^{rR_1} - 1\right)}{r - \frac{2^{R_1}(2^{rR_1} - 1)}{2^{rR_1}(2^{R_1} - 1)}}. \tag{32}$$

The RHS of the above inequality, evaluated for $R_1 = 0.5$ and $r = 4$, yields 4.3 dB. In fact, in Fig. 6 ($E_b/N_0 = 3$ dB) the MC capacity region contains the MM capacity region, while in Fig. 7 ($E_b/N_0 = 3$ dB) the MM capacity region is not contained into that of MC. The MM capacity region contains the MC capacity region only in the limiting case of a noiseless system, i.e., for $E_b/N_0 \to \infty$.

With LMMSE, MM outperform MC and VS for large α_2 and small α_1, provided that (32) is satisfied. This is an unlikely situation because a real system is expected to operate with a large number of low-rate users and a small number of high-rate users. In this case, MC and VS are distinctly better than MM, especially for low E_b/N_0 (this agrees with the experimental results of [17]).

3) On the Correct Interpretation of the Asymptotic Capacity Regions: At first glance, the fact that the capacity boundaries for MM and VS do not coincide with that of MC for $\alpha_2 \to 0$ might appear strange. In fact, for α_2 strictly equal to 0, all systems are equivalent (all reduce to a single-rate system with α_1 users per chip). However, this behavior is easily explained if we take into account that the asymptotic analysis is valid under the assumption that the number of users *in both classes* (i.e., both K_1 and K_2) goes to infinity as $L \to \infty$. Obviously, this assumption rules out the case of α_2 identically zero. The intersection of the capacity region boundaries with the horizontal and vertical axes should be interpreted as the limits for $\alpha_2 \to 0$ and for $\alpha_1 \to 0$, respectively. In other words, in the MM and VS systems, even an arbitrarily small (but positive) fraction of high-rate users per chip is sufficient to make the whole system perform worse than a single-rate low-rate system. This is due to the fact that in MM and VS the most stringent power constraint is determined by high-rate users. Therefore, the system capacity is dominated by the SINR requirement of high-rate users, even if these are a negligible fraction of the overall users.

4) Suboptimality of VS with Short-Interval Detection: Apart from the limiting case $\alpha_1 \to 0$, the VS system with LMMSE receiver and short-interval detection performs uniformly worse than VS with long-interval detection and MC.

5) Empirical SINR CDF: In order to validate our analysis, we simulated a chip and symbol synchronous system with random spreading, $L = 128$, $R_1 = 0.5$, $r = 4$, and $E_b/N_0 = 3$ dB, with MM, MC, and VS (both long- and short-interval detection). Figs. 8 and 9 show the empirical SINR cdf obtained by generating 5000 independent sets of spreading sequences, for the different systems, for SUMF and LMMSE receivers, respectively. The vertical lines indicate the SINR targets $\bar{\beta}_1 = 2^{0.5} - 1 = -3.82$ dB and $\bar{\beta}_2 = 2^2 - 1 = 4.77$ dB. In all cases, we chose (α_1, α_2) to be on the capacity region boundary, with α_1 at about half of its maximum value, and γ_1, γ_2 to be the corresponding values obtained by the optimal power control recursion.

We observe that in all cases the SINR of the actual random system with finite L is distributed around its target SINR. The SINR distribution tails for high-rate users and VS are larger, since the actual spreading gain for high-rate symbols is only $128/4 = 32$ chips.

V. CONCLUSION

We have applied the recently proposed asymptotic analysis of large CDMA system based on random spreading sequences to some design issues inspired by the current standardization of third-generation wireless mobile systems. Even though our model is very simple, it is representative of some satellite systems for personal communications and our approach might be extended to more general systems.

First, we considered the tradeoff between channel coding rate and spreading gain in order to maximize the overall system spectral efficiency of a single-rate system. The impact of channel estimation techniques based on pilot symbols and on pilot signals was taken into account. With the SUMF receiver, the two pilot schemes are equivalent, while pilot symbols yield a better spec-
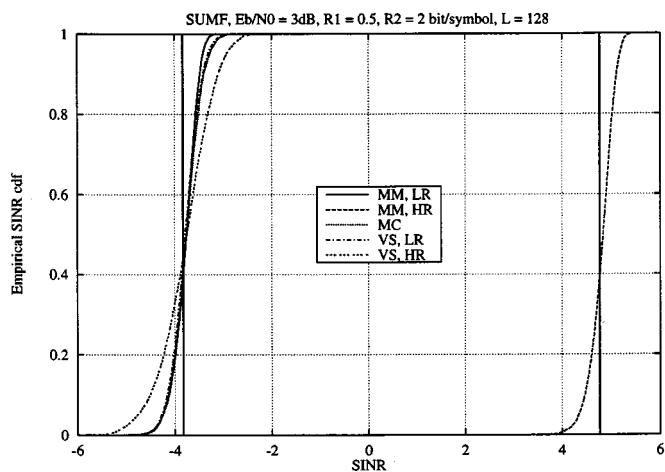
Fig. 8. Empirical SINR cdfs of MM, MC, and VS systems with SUMF receiver, for $R_1 = 0.5$ bit/symbol, $r = 4$, $E_b/N_0 = 3$ dB, and $L = 128$.
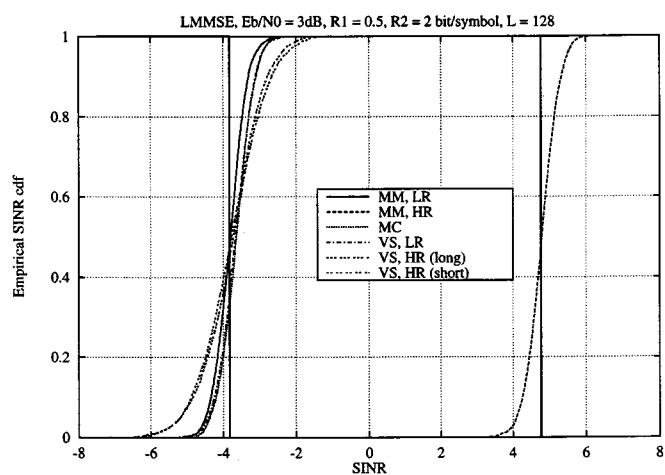

Fig. 9. Empirical SINR cdfs of MM, MC, and VS systems with LMMSE receiver, for $R_1 = 0.5$ bit/symbol, $r = 4$, $E_b/N_0 = 3$ dB, and $L = 128$.

tral efficiency than pilot signals with the LMMSE receiver. We showed that for E_b/N_0 below a given threshold (given in closed form), the system spectral efficiency is maximized by low-rate coding, no spreading, and SUMF receiver. For E_b/N_0 above this threshold, the LMMSE receiver yields larger spectral efficiency and the optimal partition between spreading gain and coding rate can be easily evaluated. This result shows that linear multiuser detection followed by single-user decoding does not provide always an improvement as far as the overall system spectral efficiency is concerned. In fact, multiuser detection should be combined with channel decoding (see, for example, the optimal MMSE decision-feedback scheme of [25] and the iterative soft interference cancellation scheme of [26]).

Then, we compared three techniques for multirate CDMA in terms of their asymptotic multirate system capacity. We showed that, with SUMF, MC and VS are equivalent, while with LMMSE, MC dominates VS. However, VS is very close to MC if high-rate users are detected by using as observation the whole low-rate symbol interval. On the contrary, if a simplified receiver using the short high-rate symbol interval is used, VS

is distinctly worse than MC. MM may perform better than MC for E_b/N_0 above a given threshold (given in closed form) and when the fraction of high-rate users is large. Monte Carlo simulation results are in close agreement with our analysis and show that the empirical cdf of the received SINR of a finite-dimensional system concentrates its probability mass around the asymptotic SINR.

APPENDIX A
PROOFS

1) VS Multirate System Model: In order to model VS multirate CDMA, we modify the basic system model (1) as

$$\mathbf{y} = \sqrt{\gamma_1} \sum_{k=1}^{K_1} \mathbf{s}_k a_k + \sqrt{r\gamma_2} \sum_{i=1}^{r} \sum_{k=1}^{K_2} \mathbf{s}_k^{(i)} a_k^{(i)} + \nu \quad (33)$$

where $\mathbf{y}$ is the received chip-rate sampled signal vector of length L during a "long" symbol interval, $\mathbf{s}_k = (1/\sqrt{L})(s_{1,k}, \ldots, s_{L,k})^T$ is the spreading sequence of the kth low-rate user, modulated by the symbol a_k

$$\mathbf{s}_k^{(i)} = \frac{1}{\sqrt{L}} \left(\underbrace{0, \ldots, 0}_{(i-1)L/r}, s_{1,k}^{(i)}, \ldots, s_{L/r,k}^{(i)}, \underbrace{0, \ldots, 0}_{(r-i)L/r} \right)^T$$

is the spreading sequence for the ith symbol of the kth high-rate user (that is nonzero only over for L/r consecutive chips), modulated by symbol $a_k^{(i)}$, and ν is the vector of complex circularly symmetric Gaussian noise samples, i.i.d. with mean zero and variance 1. Since the spreading sequences are complex random with circular symmetry, without loss of generality we have included the phase of the complex amplitude w_k in (1) as part of $\mathbf{s}_k$, and we deal only with the magnitude $|w_k| = \sqrt{\gamma_1}$ (low-rate users) and $|w_k| = \sqrt{r\gamma_2}$ (high-rate users).

With the above definitions, the receiver input vector can be written again in the compact form $\mathbf{y} = \mathbf{SWa} + \nu$, where

$$\mathbf{S} = \left[\mathbf{s}_1, \ldots, \mathbf{s}_{K_1}, \mathbf{s}_1^{(1)}, \ldots, \mathbf{s}_{K_2}^{(1)}, \ldots, \mathbf{s}_1^{(r)}, \ldots, \mathbf{s}_{K_2}^{(r)} \right]$$

is a matrix $\in \mathcal{C}^{L \times (K_1 + rK_2)}$ containing all spreading sequences by columns, $\mathbf{W}$ is a diagonal matrix given by

$$\mathbf{W} = \text{diag}(\underbrace{\sqrt{\gamma_1}, \ldots, \sqrt{\gamma_1}}_{K_1}, \underbrace{\sqrt{r\gamma_2}, \ldots, \sqrt{r\gamma_2}}_{rK_2})$$

and $\mathbf{a}$ is the vector of all modulation symbols.

Proof of Proposition 1: We make use of the following result, which can be easily obtained from the results in [4, Appendix B]. For i.i.d. random variables u_ℓ and $v_{\ell,k}$, with mean zero, variance 1, and finite fourth-order moment, the limit

$$\sum_{k=1}^{K} \left| \frac{1}{L} \sum_{\ell=1}^{L/r} u_\ell v_{\ell,k} \right|^2 \to \frac{\alpha}{r} \quad (34)$$

as $L \to \infty$ with $K/L \to \alpha$, holds in probability.

Without loss of generality, consider the output of the SUMF receiver for low-rate user 1, given by $z_1 = \mathbf{s}_1^H \mathbf{y}$. The SINR is given by

$$\beta_1^{(L)} = \frac{\gamma_1}{1 + \gamma_1 \sum_{k=2}^{K_1} \left| \mathbf{s}_1^H \mathbf{s}_k \right|^2 + r\gamma_2 \sum_{i=1}^{r} \sum_{k=1}^{K_2} \left| \mathbf{s}_1^H \mathbf{s}_k^{(i)} \right|^2}.$$

By letting $L \to \infty$, with $K_1/L \to \alpha_1$ and $K_2/L \to \alpha_2$, and by applying the limit (34), we obtain the limit in probability of $\beta_1^{(L)}$ as

$$\beta_1 = \frac{\gamma_1}{1 + \alpha_1\gamma_1 + r\gamma_2 \sum_{i=1}^{r} \frac{\alpha_2}{r}} = \frac{\gamma_1}{1 + \alpha_1\gamma_1 + r\alpha_2\gamma_2}. \tag{35}$$

Without loss of generality, we can consider the output of symbol 1 of high-rate user 1, given by $z_1^{(1)} = (\mathbf{s}_1^{(1)})^H \mathbf{y}$. By using again the limit (34), we obtain that the corresponding SINR $\beta_2^{(L)}$ converges in probability to the same limit (35). Since this is also the asymptotic SINR of a single-rate system with α_1 users/chip with SNR γ_1 and $r\alpha_2$ users/chip with SNR γ_2 (the single-rate equivalent of an MC system), we conclude that with the SUMF receiver, VS and MC are asymptotically equivalent from the SINR point of view. Since the asymptotic system capacity depends on the multirate system only through the SINR asymptotic expression, the two systems have the same capacity region.

Proof of Proposition 2: We make use of the following result of [8, Appendix A]. Let $\mathbf{A}_n \in \mathcal{C}^{n \times m_n}$ with independent complex circularly symmetric random elements $a_{i,j}$. Define the function $v_n(x,y) = nE[|a_{i,j}|^2]$, for $i/n \leq x \leq (i+1)/n$ and $j/n \leq y \leq (j+1)/n$, and assume that $v_n(x,y) < B$ for some constant $B < \infty$ independent of n, i, j. Then, as $n \to \infty$ and $m_n/n \to \alpha$, the limiting eigenvalue cdf $H(x)$ of the matrix $\mathbf{A}_n \mathbf{A}_n^H$ satisfies the integral equation

$$\int_0^\infty \frac{1}{1+tx} \, dH(x) = \int_0^1 u(x,t) \, dx \tag{36}$$

where $u(x,t)$ is the unique solution in the class of nonnegative functions, analytical on t and continuous on $x \in [0,1]$ of the integral equation

$$u(x,t) = \left(1 + t \int_0^\alpha \frac{v(x,y) \, dy}{1 + t \int_0^1 u(z,t)v(z,y) \, dz} \right)^{-1} \tag{37}$$

and where $v(x,y) = \lim_{n \to \infty} v_n(x,y)$.

Now, without loss of generality, we consider the SINR at the output of the LMMSE receiver for low-rate user 1. This is given by [4]

$$\beta_1^{(L)} = \gamma_1 \mathbf{s}_1^H \Sigma_1^{-1} \mathbf{s}_1 \tag{38}$$

where $\Sigma_1 = \mathbf{S}_1 \mathbf{W}_1 \mathbf{W}_1^H \mathbf{S}_1^H + \mathbf{I}$, $\mathbf{S}_1$ is obtained from $\mathbf{S}$ by removing the first column, and $\mathbf{W}_1$ is obtained from $\mathbf{W}$ by removing the first column and row. From [8, Lemma A.1], we know that, since Σ_1 is statistically independent of $\mathbf{s}_1$, the limit

$$\lim_{L \to \infty} \left(\mathbf{s}_1^H \Sigma_1^{-1} \mathbf{s}_1 - \frac{1}{L} \operatorname{tr}(\Sigma^{-1}) \right) = 0$$

holds in probability. The eigenvalues ξ of Σ^{-1} are related to the eigenvalues λ of $\mathbf{S}_1 \mathbf{W}_1 \mathbf{W}_1^H \mathbf{S}_1^H$ by $\xi = 1/(1+\lambda)$. Then, the limit in probability of $\beta_1^{(L)}$ as $L \to \infty$ can be written as

$$\beta_1 = \gamma_1 \int_0^\infty \frac{1}{1+\lambda} \, dG(\lambda) \tag{39}$$

where $G(\lambda)$ is the asymptotic eigenvalue distribution of $\mathbf{S}_1 \mathbf{W}_1 \mathbf{W}_1^H \mathbf{S}_1^H$.

Now, we can apply results (36) and (37) to the matrix $\mathbf{S}_1 \mathbf{W}_1$. The function $v(x,y)$ is given by

$$v(x,y) = \begin{cases} \gamma_1, & 0 \leq x \leq 1; \ 0 \leq y \leq \alpha_1 \\ r\gamma_2, & i/r \leq x < (i+1)/r \\ & \alpha_1 + i\alpha_2 \leq y < \alpha_1 + (i+1)\alpha_2 \\ & \forall i = 0, \ldots, r-1 \\ 0, & \text{elsewhere.} \end{cases}$$

By using the above expression, we can solve explicitly for the function $u(x,t)$. In fact, we have

$$
\begin{aligned}
u(x,t) &= \left[1 + t \left(\int_0^{\alpha_1} \frac{\gamma_1 \, dy}{1 + t\gamma_1 \int_0^1 u(z,t) \, dz} \right. \right. \\
&\quad \left. \left. + \sum_{i=0}^{r-1} \int_{\alpha_1+i\alpha_2}^{\alpha_1+(i+1)\alpha_2} \frac{r\gamma_2 \chi_{\{i/r \leq x < (i+1)/r\}} \, dy}{1 + tr\gamma_2 \int_{i/r}^{(i+1)/r} u(z,t) \, dz} \right) \right]^{-1} \\
&= \left[1 + t \left(\frac{\alpha_1\gamma_1}{1 + t\gamma_1 \int_0^1 u(z,t) \, dz} \right. \right. \\
&\quad \left. \left. + \sum_{i=0}^{r-1} \frac{r\alpha_2\gamma_2 \chi_{\{i/r \leq x < (i+1)/r\}}}{1 + tr\gamma_2 \int_{i/r}^{(i+1)/r} u(z,t) \, dz} \right) \right]^{-1}
\end{aligned}
\tag{40}
$$

where $\chi_{\{\mathcal{A}\}}$ denotes the indicator function of the set $\mathcal{A}$. The function $u(x,t) = \text{const.}$ for $x \in [0,1]$ is clearly a solution of the above equation for all t (the constant depends on t), and by the uniqueness of the solution of (37), it must be the only one.

From (39) and (36), by using the above result, we let $u(x,1) = u_1$ and we obtain

$$
\begin{aligned}
\beta_1/\gamma_1 &= \int_0^\infty \frac{1}{1+\lambda} \, dG(\lambda) \\
&= \int_0^1 u(x,1) \, dx \\
&= u_1 \\
&= \left[1 + \frac{\alpha_1\gamma_1}{1 + \gamma_1 u_1} + \frac{r\alpha_2\gamma_2}{1 + \gamma_2 u_1} \right]^{-1}
\end{aligned}
\tag{41}
$$

which yields (25).

Proof of Proposition 3: Without loss of generality, we consider the detection of the first symbol of high-rate user 1. In the following, given a vector $\mathbf{x}$ of length L, we denote by $\tilde{\mathbf{x}}$ the subvector of its first L/r components and by $\hat{\mathbf{x}}$ the subvector of its last $(r-1)L/r$ components, so that $\mathbf{x} = (\tilde{\mathbf{x}}^T, \hat{\mathbf{x}}^T)^T$. With short-interval detection, the receiver input is the subvector $\hat{\mathbf{y}}$. Notice that $\tilde{\mathbf{s}}_k^{(i)} = \mathbf{0}$ for all $i = 2, \ldots, r$ and all $k = 1, \ldots, K_2$.

Therefore, the SINR at the output of the LMMSE receiver is given by $\beta_2^{(L)} = r\gamma_2(\tilde{\mathbf{s}}_1^{(1)})^H\tilde{\Sigma}_1^{-1}\tilde{\mathbf{s}}_1^{(1)}$, where

$$\tilde{\Sigma}_1 = \gamma_1\sum_{k=1}^{K_1}\tilde{\mathbf{s}}_k\tilde{\mathbf{s}}_k^H + r\gamma_2\sum_{k=2}^{K_2}\tilde{\mathbf{s}}_k^{(1)}\left(\tilde{\mathbf{s}}_k^{(1)}\right)^H + \mathbf{I}.$$

Now, $\beta_2^{(L)}$ can be interpreted as the SINR of an equivalent system with spreading gain L/r, with K_1 users having SNR γ_1/r and with K_2 users having SNR γ_2. The fraction of users per chip are given by $K_1/(L/r) = r\alpha_1$ and by $K_2/(L/r) = r\alpha_2$, respectively. Since the elements of all sequences contributing to $\beta_2^{(L)}$ are i.i.d., we can apply directly the result of [4] and write the limiting SINR as

$$\begin{aligned}\beta_2 &= \frac{\gamma_2}{1 + r\alpha_1\dfrac{(\gamma_1/r)\gamma_2}{\gamma_2 + (\gamma_1/r)\beta_2} + r\alpha_2\dfrac{\gamma_2}{1+\beta_2}} \\ &= \frac{\gamma_2}{1 + \alpha_1\dfrac{\gamma_1\gamma_2}{\gamma_2 + \gamma_1\beta_2/r} + r\alpha_2\dfrac{\gamma_2}{1+\beta_2}}.\end{aligned} \quad (42)$$

Proof of Proposition 4: We use the same notation as in the previous proof, but now we consider the detection of the first symbol of high-rate user 1 over the long interval (i.e., by using the whole vector $\mathbf{y}$ as observation). The SINR at the output of the LMMSE receiver is given by

$$\beta_2^{(L)} = r\gamma_2\left(\mathbf{s}_1^{(1)}\right)^H\Sigma_1^{-1}\mathbf{s}_1^{(1)} = r\gamma_2\left(\tilde{\mathbf{s}}_1^{(1)}\right)^H\mathbf{\Phi}_{1,1}\tilde{\mathbf{s}}_1^{(1)} \quad (43)$$

where $\Sigma_1 = \mathbf{S}_1\mathbf{W}_1\mathbf{W}_1^H\mathbf{S}_1^H + \mathbf{I}$, $\mathbf{S}_1$ is obtained from $\mathbf{S}$ by removing the (K_1+1)th column, and $\mathbf{W}_1$ is obtained from $\mathbf{W}$ by removing the (K_1+1)th column and row, and where $\mathbf{\Phi}_{1,1}$ is the upper left $L/r \times L/r$ submatrix of Σ_1^{-1}. Since $\mathbf{\Phi}_{1,1}$ is statistically independent of $\tilde{\mathbf{s}}_1^{(1)}$, from [8, Lemma A.1], we have that the limit

$$\lim_{L\to\infty}\left(\left(\tilde{\mathbf{s}}_1^{(1)}\right)^H\mathbf{\Phi}_{1,1}\tilde{\mathbf{s}}_1^{(1)} - \frac{1}{r}\frac{1}{(L/r)}\text{tr}(\mathbf{\Phi}_{1,1})\right) = 0$$

holds in probability. Then, the limit in probability of $\beta_2^{(L)}$ as $L\to\infty$ can be written as

$$\beta_2 = \gamma_2\int_0^\infty \xi\,dG(\xi) \quad (44)$$

where $G(\xi)$ is the asymptotic eigenvalue distribution of $\mathbf{\Phi}_{1,1}$.

We write Σ_1 as a 2×2 block matrix with blocks $\Sigma_{1,1}, \Sigma_{1,2}, \Sigma_{1,2}^H$, and $\Sigma_{2,2}$, where $\Sigma_{1,1}$ is $L/r \times L/r$. The submatrices can be written explicitly in terms of the spreading sequences as

$$\Sigma_{1,1} = \gamma_1\sum_{k=1}^{K_1}\tilde{\mathbf{s}}_k\tilde{\mathbf{s}}_k^H + r\gamma_2\sum_{k=2}^{K_2}\tilde{\mathbf{s}}_k^{(1)}\left(\tilde{\mathbf{s}}_k^{(1)}\right)^H + \mathbf{I}$$

$$\Sigma_{1,2} = \gamma_1\sum_{k=1}^{K_1}\tilde{\mathbf{s}}_k\hat{\mathbf{s}}_k^H$$

$$\Sigma_{2,2} = \gamma_1\sum_{k=1}^{K_1}\hat{\mathbf{s}}_k\hat{\mathbf{s}}_k^H + r\gamma_2\sum_{i=2}^{r}\sum_{k=1}^{K_2}\hat{\mathbf{s}}_k^{(i)}\left(\hat{\mathbf{s}}_k^{(i)}\right)^H + \mathbf{I}. \quad (45)$$

From the matrix inversion lemma [27], we can write

$$\begin{aligned}\mathbf{\Phi}_{1,1}^{-1} &= \Sigma_{1,1} - \Sigma_{1,2}\Sigma_{2,2}^{-1}\Sigma_{1,2}^H \\ &= \Sigma_{1,1} - \gamma_1^2\sum_{k=1}^{K_1}\sum_{\ell=1}^{K_1}\left(\hat{\mathbf{s}}_k^H\Sigma_{2,2}^{-1}\hat{\mathbf{s}}_\ell\right)\tilde{\mathbf{s}}_k\tilde{\mathbf{s}}_\ell^H \\ &= \gamma_1\sum_{k=1}^{K_1}\left[1 - \gamma_1\hat{\mathbf{s}}_k^H\Sigma_{2,2}^{-1}\hat{\mathbf{s}}_k\right]\tilde{\mathbf{s}}_k\tilde{\mathbf{s}}_k^H \\ &\quad + r\gamma_2\sum_{k=2}^{K_2}\tilde{\mathbf{s}}_k^{(1)}\left(\tilde{\mathbf{s}}_k^{(1)}\right)^H + \mathbf{B}^{(L)} + \mathbf{I}\end{aligned} \quad (46)$$

where we let

$$\mathbf{B}^{(L)} = \gamma_1^2\sum_{k=1}^{K_1}\sum_{\ell\neq k}\left(\hat{\mathbf{s}}_k^H\Sigma_{2,2}^{-1}\hat{\mathbf{s}}_\ell\right)\tilde{\mathbf{s}}_k\tilde{\mathbf{s}}_\ell^H.$$

By using the same techniques of [4, Appendix B] and the matrix inversion lemma, it is not difficult to show that $\mathbf{B}^{(L)}$ converges in probability to the zero matrix, as $L\to\infty$. Now, we notice that the term

$$\epsilon_k^{(L)} = 1 - \gamma_1\hat{\mathbf{s}}_k^H\Sigma_{2,2}^{-1}\hat{\mathbf{s}}_k$$

is just the MSE resulting from LMMSE estimation of symbol the a_k of the kth low-rate user with observation $\hat{\mathbf{y}}$. We notice also that $\hat{\mathbf{y}}$ can be seen as the output of a virtual multirate system with K_1 low-rate users with spreading gain $L' = (r-1)L/r$, K_2 high-rate users with spreading gain $L'' = L/r = L'/(r-1)$ and with rate ratio $r - 1$. From Proposition 2, we know that the SINR for a low-rate user in such system converges in probability to a constant $\hat{\beta}$ independent of the particular user. Then, $\epsilon_k^{(L)}$ converges in probability to the constant $1/(1+\hat{\beta})$, as $L\to\infty$. We conclude that $\mathbf{\Phi}_{1,1}^{-1}$ is asymptotically equal (in the sense of convergence in probability) to the matrix

$$\mathbf{Q} = \frac{\gamma_1}{1+\hat{\beta}}\sum_{k=1}^{K_1}\tilde{\mathbf{s}}_k\tilde{\mathbf{s}}_k^H + r\gamma_2\sum_{k=2}^{K_2}\tilde{\mathbf{s}}_k^{(1)}\left(\tilde{\mathbf{s}}_k^{(1)}\right)^H + \mathbf{I}. \quad (47)$$

The improvement provided by long-interval detection of the high-rate users can be clearly seen from the above formula. Namely, the interfering energy of low-rate users is reduced by the factor $1/(1+\hat{\beta})$, i.e., by the MSE resulting from the estimation of low-rate users over the complement interval (where the spreading sequence of the high-rate user symbol is zero), that is ignored in the case of short-interval detection.[4]

From the fact that $\mathbf{\Phi}_{1,1}\to\mathbf{Q}^{-1}$, and by using (44) and (47), we can write

$$\beta_2 = \gamma_2\int_0^\infty\frac{1}{1+\lambda}\,dF(\lambda) \quad (48)$$

where $F(\lambda)$ is the asymptotic eigenvalue cdf of the matrix

$$\frac{\gamma_1}{1+\hat{\beta}}\sum_{k=1}^{K_1}\tilde{\mathbf{s}}_k\tilde{\mathbf{s}}_k^H + r\gamma_2\sum_{k=2}^{K_2}\tilde{\mathbf{s}}_k^{(1)}\left(\tilde{\mathbf{s}}_k^{(1)}\right)^H.$$

Since all sequences appearing in the above expression have i.i.d. entries, by following the same path of [4, Sec. 4], we obtain that β_2 must satisfy (27).

[4]In fact, if $\hat{\beta} = 0$, $\mathbf{Q}$ becomes identical to $\bar{\Sigma}_1$ defined in the proof of Proposition 3 (short-interval detection).

In order to complete the proof of Proposition 4, we have to show that $\hat{\beta}$ must satisfy (28). This is immediately obtained by applying Proposition 2 to the new multirate system with output $\hat{\mathbf{y}}$. We skip the details for the sake of space limitation.

Proof of Proposition 5: Consider the equations

$$x = \frac{\gamma_1}{1 + \alpha_1 \dfrac{\gamma_1}{1+x} + r\alpha_2 \dfrac{\gamma_1\gamma_2}{\gamma_1+\gamma_2 x}} \tag{49}$$

$$x = \frac{\gamma_2}{1 + \alpha_1 \dfrac{\gamma_1\gamma_2}{\gamma_2+\gamma_1 x} + r\alpha_2 \dfrac{\gamma_2}{1+x}} \tag{50}$$

$$x = \frac{\gamma_2}{1 + \alpha_1 \dfrac{\gamma_1\gamma_2}{\gamma_2(1+\hat{\beta})+\gamma_1 x/r} + r\alpha_2 \dfrac{\gamma_2}{1+x}} \tag{51}$$

$$x = \frac{\gamma_2}{1 + \alpha_1 \dfrac{\gamma_1\gamma_2}{\gamma_2+\gamma_1 x/r} + r\alpha_2 \dfrac{\gamma_2}{1+x}} \tag{52}$$

where $\hat{\beta}$ satisfy (28). The (unique nonnegative) solution x_1 of (49) yields the asymptotic SINR β_1 for low-rate users in both the MC and the VS systems, while the solutions x_2, x_3, x_4 of (50)–(52) yield the asymptotic SINR β_2 for high-rate users in the MC, VS (long-interval detection), and VS (short-interval detection) systems, respectively. Let

$$\begin{aligned} y_1 &= \sup_{\gamma_1\leq\bar{\gamma}_1, \gamma_2\leq\bar{\gamma}_1} \min\{x_1, x_2\} \\ y_2 &= \sup_{\gamma_1\leq\bar{\gamma}_1, \gamma_2\leq\bar{\gamma}_1} \min\{x_1, x_3\} \\ y_3 &= \sup_{\gamma_1\leq\bar{\gamma}_1, \gamma_2\leq\bar{\gamma}_1} \min\{x_1, x_4\} \end{aligned} \tag{53}$$

for given $r > 1$ and α_1, α_2. Since the SINR requirement is the same (i.e., $\beta_1 \geq \bar{\beta}_1$ and $\beta_2 \geq \bar{\beta}_1$) for both low-rate and high-rate users, and because of the monotonicity of the interference function with respect to $\bar{\beta}_1$, the inclusion relations between the capacity regions of these systems stated in Proposition 5 follow by showing that $y_1 \geq y_2 \geq y_3$.

First, we observe that if $\gamma_1 = \gamma_2$, then $x_1 = x_2$, therefore y_1 is trivially obtained by letting $\gamma_1 = \gamma_2 = \bar{\gamma}_1$. Since $r > 1$ and $\hat{\beta} \geq 0$, $x_4 \leq x_3$, and $x_4 \leq x_2$ for all γ_1, γ_2. It follows that $\mathcal{R}^{\mathrm{MC}} \supseteq \mathcal{R}^{\mathrm{VS,short}}$ and that $\mathcal{R}^{\mathrm{VS,long}} \supseteq \mathcal{R}^{\mathrm{VS,short}}$. It remains to show that $\mathcal{R}^{\mathrm{MC}} \supseteq \mathcal{R}^{\mathrm{VS,long}}$ (i.e., that $y_1 \geq y_2$). Consider (28) yielding $\hat{\beta}$. We substitute $X = (r/r - 1)\hat{\beta}$ into (28) and we obtain

$$\begin{aligned} X &= \frac{\gamma_1}{1 + \alpha_1 \dfrac{\gamma_1}{1+\frac{r-1}{r}X} + r\alpha_2 \dfrac{\gamma_1\gamma_2}{\gamma_1+\gamma_2 X}} \\ &\leq \frac{\gamma_1}{1 + \alpha_1 \dfrac{\gamma_1}{1+X} + r\alpha_2 \dfrac{\gamma_1\gamma_2}{\gamma_1+\gamma_2 X}}. \end{aligned} \tag{54}$$

From (54) and (49), we conclude that $\hat{\beta} \leq (r - 1/r)x_1$, for all $\gamma_1, \gamma_2, \alpha_1, \alpha_2$, and $r > 1$. Let x'_3 be the solution of (51) when we replace $\hat{\beta}$ by $(r - 1/r)x_1$, and let $y'_2 = \sup_{\gamma_1\leq\bar{\gamma}_1, \gamma_2\leq\bar{\gamma}_1} \min\{x_1, x'_3\}$. Since $x'_3 \geq x_3$ (this follows form the fact that $\hat{\beta} \leq (r - 1/r)x_1$, as shown before), then $y'_2 \geq y_2$. Now, it is not difficult to show that $y'_2 = y_1$, and it is obtained for $\gamma_1 = \gamma_2 = \bar{\gamma}_1$. This concludes the proof.

APPENDIX B
COMPARISON OF THE CAPACITY REGIONS OF MULTIMODULATION AND MULTICODE WITH THE LMMSE RECEIVER

The capacity regions with the LMMSE receiver are described by inequalities (20) and (24) in the cases of MM and MC, respectively. For a fair comparison, we assume that $\gamma_2 = r\gamma_1 = rR_1E_b/N_0$. The analysis of the capacity region is simplified if we observe that

$$\begin{aligned} \bar{\beta}_2 &= 2^{R_2} - 1 \\ &= 2^{rR_1} - 1 \\ &= [1 + (2^{R_1} - 1)]^r - 1 > r(2^{R_1} - 1) \\ &= r\bar{\beta}_1 \end{aligned}$$

and hence $1 - \bar{\beta}_2/\bar{\gamma}_2 < 1 - \bar{\beta}_1/\bar{\gamma}_1$ for all $r > 1$. Inequalities (20) and (24) can be written as in the equation shown at the bottom of the page.

1) Intersection of the α_1 Axis: It is clear from the above equations that the intersection of the α_1 axis with MM (obtained by setting $\alpha_2 = 0$ above) is always lower than the corresponding intersection with MC.

2) Slopes of the Capacity Boundaries: The (absolute) slope of the MC capacity boundary is always smaller than the slope of the MM capacity boundary, or, equivalently

$$\frac{\bar{\beta}_2(1+\bar{\beta}_1)}{\bar{\beta}_1(1+\bar{\beta}_2)} < r.$$

This can be shown as follows:

$$\begin{aligned} \frac{\bar{\beta}_2(1+\bar{\beta}_1)}{\bar{\beta}_1(1+\bar{\beta}_2)} < r &\Leftrightarrow 1 + \frac{1}{\bar{\beta}_1} < r + \frac{r}{\bar{\beta}_2} \\ &\Leftrightarrow 1 + \frac{1}{2^{R_1}-1} < r + \frac{r}{2^{rR_1}-1} \\ &\Leftrightarrow 2^{R_1}(2^{rR_1}-1) < r2^{rR_1}(2^{R_1}-1) \\ &\Leftrightarrow 0 < (r-1)(2^{rR_1}-1)(2^{R_1}-1) \end{aligned}$$

and the last inequality trivially holds.

$$\begin{cases} \alpha_1 + \dfrac{\bar{\beta}_2(1+\bar{\beta}_1)}{\bar{\beta}_1(1+\bar{\beta}_2)}\alpha_2 \leq \dfrac{1+\bar{\beta}_1}{\bar{\beta}_1}\left(1 - \dfrac{\bar{\beta}_2}{\bar{\gamma}_2}\right) < \dfrac{1+\bar{\beta}_1}{\bar{\beta}_1}\left(1 - \dfrac{\bar{\beta}_1}{\bar{\gamma}_1}\right) & \text{(MM)} \\ \alpha_1 + r\alpha_2 \leq \dfrac{1+\bar{\beta}_1}{\bar{\beta}_1}\left(1 - \dfrac{\bar{\beta}_1}{\bar{\gamma}_1}\right) & \text{(MC)} \end{cases}$$

3) Intersection of the Capacity Boundaries: The boundaries of the MM and MC capacity regions may intersect since the (absolute) slope of MM is higher than that of MC. Solving the linear equations defining the boundaries, we get

$$\alpha_1 = \frac{1}{r - \bar{\beta}_2(1+\bar{\beta}_1)/(\bar{\beta}_1(1+\bar{\beta}_2))}$$
$$\times \left[r\left(1 - \frac{\bar{\beta}_2}{\bar{\gamma}_2}\right) - \frac{\bar{\beta}_2(1+\bar{\beta}_1)}{\bar{\beta}_1(1+\bar{\beta}_2)}\left(1 - \frac{\bar{\beta}_1}{\bar{\gamma}_1}\right) \right].$$

The intersection is in the capacity region provided that $\alpha_1 \geq 0$, i.e., provided that (32) is satisfied.

ACKNOWLEDGMENT

REFERENCES

[1] A. J. Grant and P. D. Alexander, "Randomly selected spreading sequences for coded CDMA," in *Proc. 4th Int. Symp. Spread Spectrum Tech. Appl. (ISSSTA'96)*, Mainz, Germany, Sept. 22–25, 1996, pp. 54–57.

[2] S. Verdú and S. Shamai (Shitz), "Multiuser detection with random spreading and error correction codes: Fundamental limits," in *Proc. 1997 Allerton Conf. Commun., Contr. and Comp.*, Urbana, IL, Sept.–Oct. 1997.

[3] ——, "Spectral efficiency of CDMA with random spreading," *IEEE Trans. Inform. Theory*, vol. 45, pp. 622–640, Mar. 1999.

[4] D. Tse and S. Hanly, "Linear multiuser receivers: Effective interference, effective bandwidth and capacity," *IEEE Trans. Inform. Theory*, vol. 45, pp. 641–657, Mar. 1999.

[5] D. Tse and S. V. Hanly, "Network capacity, power control, and effective bandwidth," in *Wireless Communications: Signal Processing Perspectives*. ser. Signal Processing Series, H. V. Poor and G. W. Wornell, Eds. Englewood Cliffs, NJ: Prentice-Hall, 1998.

[6] V. L. Girko, *Theory of Random Determinants*. New York: Kluwer, 1990.

[7] S. Verdú, *Multiuser Detection*. Cambridge, U.K.: Cambridge Univ. Press, 1998.

[8] D. Tse, "Effective interference and effective badwidth of linear multiuser receivers in asynchronous systems," IEEE Trans. Inform. Theory, vol. 46, pp. 1426–1447, July 2000, to be published.

[9] S. Shamai (Shitz) and S. Verdú, "The effect of frequency-flat fading on the spectral efficiency of CDMA," IEEE Trans. Inform. Theory, submitted for publication.

[10] J. Evans and D. Tse, "Large system performance of linear multiuser receivers in multipath fading channels," IEEE Trans. Inform. Theory, submitted for publication.

[11] D. Tse and S. Verdú, "Optimum multiuser asymptotic efficiency of CDMA with random spreading," in *IEEE Information Theory Workshop on Detection, Estimation, Classification and Imaging*, Santa Fe, NM, Feb. 24–26, 1999.

[12] E. Tiedemann, Y.-C. Jou, and J. Odenwaalder, "The evolution of IS-95 to a third generation system and to the IMT-2000 era," in *Proc. ACTS Summit*, Aalborg, Denmark, Oct. 1997, pp. 924–929.

[13] E. Dahlman, B. Gudmundson, M. Nilsson, and J. Sköld, "UMTS/IMT-2000 based on wideband CDMA," *IEEE Commun. Mag.*, vol. 36, pp. 70–81, Sept. 1998.

[14] "Robust Modulation and Coding for Personal Communication Systems," Eur. Space Agency, Final Rep., Contract 12 497/NL/97/NB.

[15] G. Caire, R. De Gaudenzi, G. Gallinaro, R. Lyons, M. Luglio, M. Ruggieri, A. Vernucci, and H. Widmer, "ESA satellite wideband CDMA radio transmission technology for the IMT-2000/UMTS satellite component: Features & performance," in *GLOBECOM'99*, Rio de Janeiro, Brazil, Dec. 5–7, 1999.

[16] J. Chen and U. Mitra, "MMSE Receivers for dual-rate synchronous DS/CDMA systems: Random signature sequence analysis," in *Proc. IEEE GLOBECOM'97, Communication Theory Mini-Conf.*, Phoenix, AZ, Nov. 1997.

[17] T. Ottosson, "Coding, Modulation and Multiuser Decoding for DS-CDMA Systems," Ph.D. dissertation, Chalmers Univ. Technol., Sweden, 1997.

[18] F. Adachi, K. Ohno, A. Higashi, T. Dohi, and Y. Okumura, "Coherent multicode DS-CDMA mobile radio access," *IEICE Trans. Commun.*, vol. E79-B, no. 9, pp. 1316–1325, Sept. 1996.

[19] F. Adachi, M. Sawahashi, and K. Okawa, "Spreading codes with different lengths for forward link of DS-CDMA mobile radio," *Electron. Lett.*, vol. 33, pp. 27–28, Jan. 2nd, 1997.

[20] J. Proakis, *Digital Communications*, 3rd ed. New York: McGraw-Hill, 1995.

[21] P. Frenger, P. Orten, and T. Ottosson, "Code-spread CDMA using maximum free distance low-rate convolutional codes," IEEE Trans. Commun., vol. 48, pp. 135–144, Jan. 2000, to be published.

[22] S. Miller, M. Honig, and L. Milstein, "Performance analysis of MMSE receivers for DS-CDMA in frequency selective fading channels," IEEE Trans. Commun., submitted for publication.

[23] R. Yates, "A framework of uplink power control in cellular radio systems," *IEEE J. Select. Areas Commun.*, vol. 13, pp. 1341–1347, Sept. 1995.

[24] T. Cover and J. Thomas, *Elements of Information Theory*. New York: Wiley, 1991.

[25] M. Varanasi and T. Guess, "Optimum decision feedback multiuser equalization with successive decoding achieves the total capacity of the Gaussian multiple-access channel," in *35th Asilomar Conf. Signals, Systems, Computers*, Pacific Groove, CA, Nov. 2–5, 1997.

[26] X. Wang and V. Poor, "Iterative (Turbo) soft interference cancellation and decoding for coded CDMA," *IEEE Trans. Commun.*, vol. 47, pp. 1046–1061, July 1999.

[27] R. Horn and C. Johnson, *Matrix Analysis*. Cambridge, U.K.: Cambridge Univ. Press, 1985.

Ezio Biglieri (M'73–SM'82–F'89) was born in Aosta, Italy. He studied electrical engineering at Politecnico di Torino, Torino, Italy, where he received the Dr. Engr. degree in 1967.

From 1968 to 1975, he was with the Istituto di Elettronica e Telecomunicazioni, Politecnico di Torino, first as a Research Engineer, then as an Associate Professor (jointly with Istituto Matematico). In 1975, he was appointed Professor of Electrical Engineering at the University of Napoli, Italy. In 1977, he returned to Politecnico di Torino as a Professor in the Department of Electrical Engineering. From 1987 to 1989, he was a Professor of Electrical Engineering at the University of California at Los Angeles (UCLA). Since 1990, he has been again a Professor with Politecnico di Torino. He has held visiting positions with the Department of System Science, UCLA, the Mathematical Research Center, Bell Laboratories, Murray Hill, NJ, Bell Laboratories, Holmdel, NJ, the Department of Electrical Engineering, UCLA, the Telecommunication Department of L'Ecole Nationale Supérieure des Télécommunications, Paris, France, the University of Sydney, Australia, the Yokohama National University, Japan, and the Electrical Engineering Department of Princeton University, Princeton, NJ. He has edited three books and co-authored five, among which the most recent is *Principles of Digital Transmission with Wireless Applications* (New York: Kluwer/Plenum, 1999).

In 1988, 1992, and 1996, Dr. Biglieri was elected to the Board of Governors of the IEEE Information Theory Society, in which he served as President in 1999. From 1988 to 1991, he was an Editor for IEEE TRANSACTIONS ON COMMUNICATIONS, and from 1991 to 1994, an Associate Editor for IEEE TRANSACTIONS ON INFORMATION THEORY. Since 1997, he has been an Editor for IEEE COMMUNICATIONS LETTERS, and the Editor-in-Chief of the *European Transactions on Telecommunications*, and since 1998, a Division Editor of the *Journal on Communications and Networks*. In 2000, he received the IEEE Third Millennium Medal and the IEEE Donald G. Fink Prize Paper Award.

Giuseppe Caire (S'91–M'94) was born in Torino, Italy, on May 21, 1965. He received the B.Sc. degree in electrical engineering from Politecnico di Torino, Torino, Italy, in 1990, the M.Sc. degree in electrical engineering from Princeton University, Princeton, NJ, in 1992, and the Ph.D. degree from Politecnico di Torino in 1994.

Currently, he is Associate Professor with the Department of Mobile Communications at the Institute Eurecom, Sophia-Antipolis, France. He was Assistant Professor in Telecommunications at the Politecnico di Torino from 1994 to 1998. He was with the European Space Agency (ESTEC), Noordwijk, The Netherlands, in 1995, the Institute Eurecom, Sophia Antipolis, France, in 1996, and Princeton University, Princeton, NJ, in the summer of 1997. He is co-author of more than 30 papers in international journals and more than 60 papers in international conferences, and he is author of three international patents with the European Space Agency. His interests are focused on digital communications theory, information theory, coding theory and multiuser detection, with particular focus on wireless terrestrial and satellite applications.

Dr. Caire is Associate Editor for CDMA and Multiuser Detection of the IEEE TRANSACTIONS ON COMMUNICATIONS and Associate Editor for Communication Theory of the *Journal of Communications and Network* (JCN). He was a recipient of the AEI G. Someda Scholarship in 1991, the COTRAO Scholarship in 1996, and a CNR Scholarship in 1997.

Giorgio Taricco (M'91) was born in Torino, Italy, in 1961. He received training in electrical engineering from Politecnico di Torino, Torino, Italy, where he received the Dr.Engr. degree in 1985.

From 1985 to 1987, he was with CSELT (Italian Telecom Laboratories) working on the design and definition of the GSM communication system with special regard to the performance of the channel coding subsystem. Since 1991, he has been with the Dipartimento di Elettronica of Politecnico di Torino, Torino, Italy, where he is a Professor of Analog and Digital Communications. In 1996, he was a Research Fellow at ESTEC. Currently, he is co-author of about 40 papers in international journal and 80 conference works. His research intersests are in the areas of error-control coding, digital communications, multiuser detection and information theory with applications to mobile communication systems.